

Atomic Bose-Einstein condensates in optical lattices with variable spatial symmetry

Sebastian Kling, Tobias Salger, Carsten Geckeler, Gunnar Ritt, Johannes Plumhof, and Martin Weitz

Institut für Angewandte Physik der Universität Bonn, Wegelerstr. 8, D-53115 Bonn

1.1 Abstract

We report on experiments studying quantum transport of an atomic Bose-Einstein condensate in variable periodic potentials. For the generation of high spatial periodicity lattices, we use the dispersion of higher order multiphoton Raman transitions. With an n -th order Raman transition, a lattice potential of spatial periodicity $\lambda/2n$ is obtained. Further, by combination of lattices with different spatial periodicities, in principle arbitrarily shaped periodic potentials can be Fourier-synthesized. In particular, we have investigated the band structure of the superposition of a conventional lattice with $\lambda/2$ spatial periodicity and a $\lambda/4$ periodicity multiphoton lattice. Depending on the relative phase of the spatial harmonics, both symmetric and sawtooth-like asymmetric potentials can be synthesized. We experimentally find that the Landau-Zener tunneling rate between the first and second excited Bloch band depends on the phase between the spatial lattice harmonics. For the future, we expect that a study of quantum transport in driven sawtooth-like ratchet potentials will allow for novel quantum dynamical phenomenon, such as an investigation of the Hamiltonian ratchet regime.

1.2 Introduction

Optical lattices for atomic Bose-Einstein condensates raised enormous interest, as they mirror features known from solid state physics to the field of atom optics. In perfect solid state crystals atoms are arranged in a regular array creating a periodic potential for the electrons inside. Felix Bloch was one of the first who investigated in his dissertation (1928) the quantum mechanics of individual electrons in such crystalline solids. In the independent electron approximation interatomic and interelectronic interactions are neglected. Each electron obeys the one electron Schrödinger equation with a periodic potential

$V(\mathbf{x} + \mathbf{a}) = V(\mathbf{x})$ with period \mathbf{a} . According to Bloch's theorem the stationary eigenstates $\psi_{n,\mathbf{q}}(\mathbf{r})$ are plane waves modulated by a periodic function revealing the periodicity of the atom lattice [1]. With proper periodicity and boundary conditions the eigenstates are quantized, characterized by the band index $n = 0, 1, \dots$. The plane waves propagate in the direction of the wave vector \mathbf{q} with the associated quasi momentum $\hbar\mathbf{q}$, which it is sometimes referred to as the crystal or lattice momentum. The energy levels $E_n(\mathbf{q})$ are periodic continuous functions of the wave vector \mathbf{q} forming the energy bands. Pictures of the energy bands showing the bandstructure are conventionally restricted to the first Brillouin-zone of the reciprocal lattice $\hbar k \leq q \leq \hbar k$. One milestone of Bloch theory and the band structure of particles is the finding of a natural physical explanation of the some 20 orders of magnitude difference in electrical conductivity between an insulator and a good conductor [2].

A realization of the fundamental concept of Bloch theory more recently became also accessible in a field quite different from solid state physics, namely in quantum optics. Due to the breakthrough of creating atomic Bose-Einstein condensates in 1995 [3, 4] it is now also possible to investigate condensates confined in periodic optical potentials, so called optical lattices. Ultracold atoms exposed to such periodic potentials exhibits analogies to electrons in solids. In recent years, atoms confined in lattice potentials have allowed for observations of Bloch oscillations and Landau-Zener tunneling [5, 6], number squeezing [7], or the Mott-insulator transition [8]. Further, fascinating pictures of cubic clouds depicting the first Brillouin-zone [9] and interference patterns of Bragg scattered atoms were taken [10]. These first experiments demonstrated that optical lattices are an attractive tool for modelling effects known or predicted in solid state physics.

So far, the band structure was investigated only for sinusoidal lattice potentials, in which the lattice periodicity is given by $\lambda/2$, where λ denotes the wavelength of the used laser radiation. Other potential shapes were realized: some authors studied superlattices based on the spatial beating of two neighboring trapping sites [11, 12], others used a grey optical lattice configuration to realize asymmetric, dissipative potentials [13]. We here describe work realizing dissipationless lattice potential with spatial periodicity $\lambda/4$, which is realized with a fourth-order Raman process. Building upon this potential, a Fourier-synthesis of lattice potentials for a ^{87}Rb Bose-Einstein condensate is demonstrated. By superimposing the $\lambda/4$ period multiphoton potential with a conventional lattice potential with $\lambda/2$ spatial periodicity of appropriate phase, either symmetric or saw-tooth like asymmetric lattice potentials are synthesized. The scheme is scalable, in principle, to arbitrarily many Fourier components. In subsequent experiments, we have studied quantum transport in such lattices of variable symmetry. We find that the Landau-Zener tunneling rate of atoms between the lowest two excited Bloch bands depends on the shape of the lattice potential. In this way, the band structure of Fourier-synthesized lattices was explored.

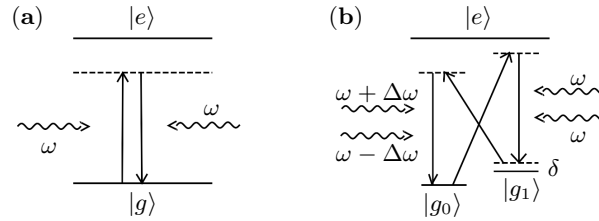


Fig. 1.1. *Virtual process in optical lattices.* (a) The trapping potential of conventional standing wave lattices is due to a virtual two photon process of absorbing and instantaneously emitting a photon of energy $\hbar\omega$. This yields the well-known spatial periodicity of $\lambda/2$. (b) Virtual four photon process contributing to a lattice potential of $\lambda/4$ spatial periodicity.

The outline is as follows: In Sect. 1.3 we describe our method to generate nonstandard optical lattices. The experimental set up is presented in Sect. 1.4 and experimental results in Sect. 1.5. We conclude this article with Sect. 1.6, where we give an outlook on quantum ratchets.

1.3 Principle of optical multiphoton lattices

A conventional lattice with sinusoidal shape and spatial periodicity $\lambda/2$ is generated by overlapping two counterpropagating off-resonant laser beams with frequency ω forming a standing wave. Due to a spatial varying ac-Stark shift, atoms experience a dipole force depending on the sign of the polarizability, which attracts the atoms to the nodes ($\omega > \omega_0$) or the anti-nodes ($\omega < \omega_0$) of the laser intensity, where ω_0 is an atomic resonance frequency. The effective potential for an atom exposed to a standing optical wave may also be described in a quantum picture by the exchange of photons changing the atom's momentum. The atoms here undergo virtual two-photon processes of absorption of one photon from one laser beam and stimulated emission of another photon into a counterpropagating beam, see Fig. 1.1a. An atom undergoing such a two photon process exchanges a momentum amount of $2\hbar k$ with the lattice.

We use a multiphoton Raman technique to generate a lattice potential of periodicity $\lambda/4$, as the first harmonic for a Fourier-synthesis of lattice potentials [14,15]. The scheme uses three-level atoms with two stable ground states $|g_0\rangle$ and $|g_1\rangle$ and the electronically excited state $|e\rangle$. The atoms are irradiated by two optical beams of frequencies $\omega + \Delta\omega$ and $\omega - \Delta\omega$ from the left and by a beam of frequency ω from the right, as shown in Fig. 1.1b. Momentum is transferred to the atoms in units of $4\hbar k$ during an induced virtual four-photon processes, being a factor two above the corresponding process in a standing

wave. This suggests a spatial periodicity of $\lambda/4$ for the adiabatic light shift potential, which is in agreement with theoretical predictions.

This scheme can be extended to generate lattice potentials with higher periodicities $\lambda/2n$ by a $2n$ -th photon process. The high resolution of Raman spectroscopy between two stable ground states over an excited state allows to clearly separate in frequency space the desired $2n$ -th order process from lower order contributions.

By combining lattice potentials of different spatial periodicities, variable periodic potentials can be synthesized [16]. At present, we experimentally investigate ratchet-type asymmetric and symmetric potentials by combining four-photon potentials based on the scheme of Fig. 1.1b with usual standing wave lattice potentials. The adiabatic lattice has then the form

$$V(z) = V_1 \cos(2kz) + V_2 \cos(4kz + \phi), \quad (1.1)$$

where V_1 and V_2 are the potential depths of the lattice potentials with spatial periodicities $\lambda/2$ and $\lambda/4$ respectively, and ϕ denotes the relative phase between the spatial harmonics. A constant offset to the potential V is here omitted. Figure 1.2a shows the form of such a lattice potential for typical experimental potential depths for a relative phase between lattice harmonics of $\phi = 0$ (solid line) and $\phi = 90^\circ$ (dashed line), as an example for a symmetric and asymmetric lattice respectively. Figure 1.2b shows the corresponding band structure for those potentials for the lowest Bloch bands. Notably, the band gap between first and second excited Bloch band depends on the phase ϕ and the potential depths V_1, V_2 of the two lattice harmonics. For given values of the potential depths V_1 and V_2 one finds, that the gap takes its maximum for $\phi = 0^\circ$ and minimum for $\phi = 180^\circ$. For a suitable choice of the lattice depths V_1, V_2 and the phase ϕ between them the gap can even vanish.

1.4 Experimental approach

Our experimental set-up was described in detail in Ref. [17]. Briefly, a ^{87}Rb Bose-Einstein condensate is produced all-optically by evaporative cooling in a CO_2 -laser dipole trap. The used evaporation time is about 10 s, during which an additional magnetic field gradient is activated, to end up with a spin-polarized condensate of about 16 000 atoms in the $|F = 1, m_F = -1\rangle$ ground state is produced.

A magnetic bias field generates a frequency splitting of $\omega_Z \simeq 2\pi \cdot 805 \text{ kHz}$ between neighbouring Zeeman ground states. The direction of the magnetic field forms an angle respectively to the optical beam, so that atoms experience σ^+ -, σ^- - and π -polarized light simultaneously. For the multiphoton lattice potential according to the scheme of Fig. 1.1b, the $F = 1$ ground state components $m_F = -1$ and 0 are used as states $|g_0\rangle$ and $|g_1\rangle$, while the

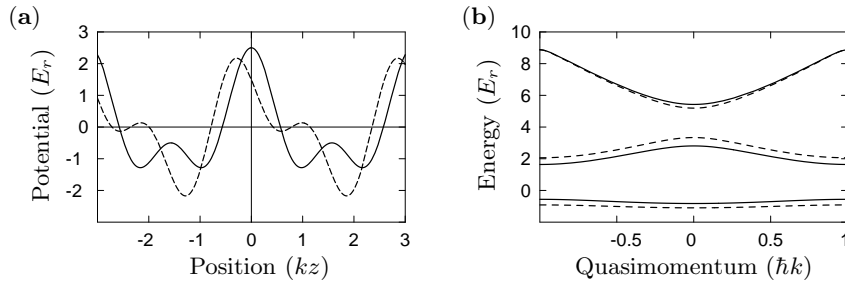


Fig. 1.2. *Lattice potential and band structure.* (a) For the experimentally realized values we show the lattice potential (1.1) for two specific phases ϕ . The solid line corresponds to $\phi = 0^\circ$ and the dashed line to $\phi = 90^\circ$. The depths are $V_1 = 3/2 E_r$ and $V_2 = 1 E_r$, where $E_r = \hbar^2 k^2 / 2M$ denotes the recoil energy, M the atomic mass. (b) Bandstructure corresponding to the lattice potentials shown in (a). It is clearly visible that the energy gap between first and second excited Bloch band depends on the phase ϕ .

$|5P_{3/2}\rangle$ manifold serves as the excited state $|e\rangle$. The Raman detuning δ typically is tuned to $2\pi \cdot 50$ kHz. The lattice beams are provided by a tapered diode laser tuned some 2 nm to the red of the rubidium D2-line. The beam is splitted into two, whereafter each of the partial beams pass an acoustooptical modulator. The modulators control the intensities and frequencies of the beams, as is required to generate superpositions of a standing wave and a four-photon potential [16]. The modulators are driven by four phase-locked rf function generators. The optical lattice beams are directed onto the ^{87}Rb condensate under an angle of 49° relatively to axis of gravity via optical fibers in a counterpropagating geometry.

1.5 Measurements and results

In initial work, we have characterized the generated lattice potentials by diffracting the atomic Bose-Einstein condensate off the variable lattice potentials. Figure 1.3 shows the result of such measurements [16], where atoms were diffracted off a $6 \mu\text{s}$ long pulse of the lattice potential, where the used free expansion time was 10 ms for the shown time-of-flight images (top figures). For both Figs. 1.3a and 1.3b, $\lambda/2$ and $\lambda/4$ periodicity lattice potentials respectively were investigated, where the smaller spatial periodicity of the multiphoton potential results in larger spatial separation of the diffracted peaks in the latter image. Figures 1.3c and 1.3d show the results obtained when combining lattice potentials of periodicity $\lambda/2$ and $\lambda/4$ for different values of the relative phase between spatial harmonics. The asymmetry of the observed diffraction images is attributed to as evidence for the asymmetry of the Fourier-synthesized lattice potentials. The shown plots below the time-of-flight images give the reconstructed lattice potentials respectively, obtained

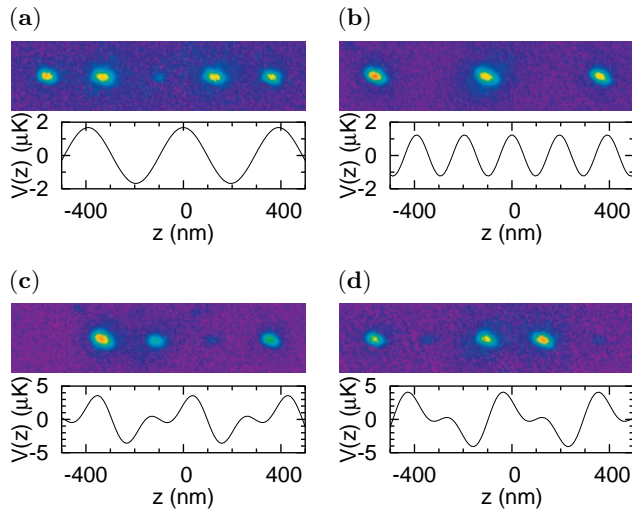


Fig. 1.3. Far-field diffraction images of lattice potentials and corresponding reconstructed spatial structure of the lattice potentials. (a) For a two-photon lattice potential with $\lambda/2$ spatial periodicity and (b) for a four-photon lattice potential with $\lambda/4$ spatial periodicity, the splitting of the clouds is a factor two above that observed in (a). (c) Diffractions image for an asymmetric lattice potential realized by superimposing two- and four-photon lattice potentials. (d) Same as in (c), but with an additional phase shift of 180° for the four-photon lattice potential.

by fitting the results of the diffraction experiment to the solution of a numerical integration of the momentum-picture Schrödinger equation [16]. More recently, we have experimentally investigated the band structure of Fourier-synthesized lattice potentials by means of quantum transport experiments. One fundamental quantum effect is Landau-Zener tunneling which can occur in accelerated lattices [18]. When the acceleration of the lattice is sufficiently large, transitions between different energy bands become possible, which is called Landau-Zener tunneling. On the other hand, for sufficiently small acceleration the atoms are Bragg diffracted at the Brillouin zone edge and the atomic quasimomentum oscillates within the Bloch bands from $-\hbar k$ to $\hbar k$, which is known as Bloch oscillation. The Landau-Zener transition probability can be estimated as [19, 20]

$$P(a) = \exp(-\pi E_G^2 / \hbar^2 k a), \quad (1.2)$$

where a is the acceleration of the lattice and E_G is the energy gap between two bands. In a series of experiments we have investigated the Landau-Zener tunneling rate between the first and the second excited Bloch band [21]. One of the lattice beams with frequency ω is used both for the standing wave and the fourth order multiphoton potential. This beam was acoustooptically

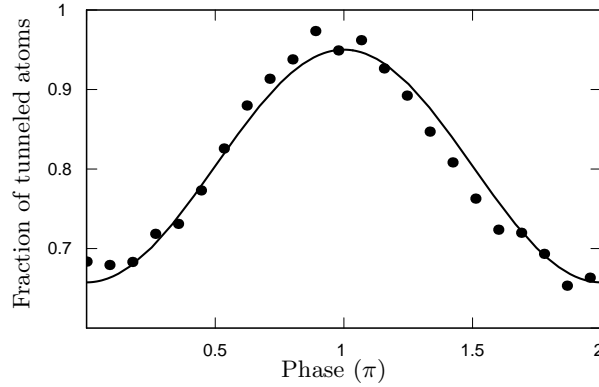


Fig. 1.4. Phase dependence of Landau-Zener tunnel rate. Shown is the ratio N_{LZ}/N of the number of atoms that have undergone a Landau-Zener transition N_{LZ} and the total number of atoms in the condensate N as a function of the phase ϕ between the two lattice harmonics of the potential (1.1). The experimental data (dots) is fitted to a sinusoidal curve (solid line).

detuned by a small amount δ_{Dopp} , so that the reference frame in which the lattice is stationary moves with a velocity of $v_{\text{rel}} = \lambda\delta_{\text{Dopp}}/4\pi$. The atoms were loaded into the first Bloch band by adiabatically transferring them into a lattice moving at a velocity $v_{\text{rel}} \simeq 1.5 \hbar k/M$, where M is the atomic mass. To accelerate the lattice we increase the beam detuning δ_{Dopp} with a constant rate, so that an acceleration is achieved which can be larger than the projection of gravity's acceleration on the lattice direction. The tunneling rate depends on the size of the band gap and therefore on the phase ϕ between the two lattice harmonics. The dependence on the phase is measured and depicted in Fig. 1.4 for an acceleration of 6.44 m/s^2 and potential depth of $V_1 \simeq 3/2 E_r$ and $V_2 \simeq 1 E_r$, where $E_r = \hbar^2 k^2/2M$ denotes the recoil energy. The data fits well to a sinusoidal curve which is fitted to the data (solid line) to guide the eyes. In the course of the experiment we studied also the dependence of the tunneling rate on the depths of the two lattice harmonics for which we refer the reader to [21]. Remarkably, for symmetric potentials $\phi = 0^\circ$ ($\phi = 180^\circ$) the Landau-Zener tunneling rate reaches a minimum (maximum) while for the ratchet type asymmetric potential ($\phi = 90^\circ$) an intermediate value is obtained. This is in contrast to dissipative asymmetric lattices, where maxima and minima tunneling rates are reached for ratchet-like potentials of different symmetry respectively.

1.6 Outlook: Quantum ratchets

A mechanical ratchet is a device used to restrict arbitrary motion into one direction. One familiar macroscopic application is the self-winding wristwatch,

where the clockwork is rewound by an eccentric weight that rotates to the movement of the wearer's body [22]. Converting microscopic fluctuations, such as Brownian motion, into useful work was suggested by Smoluchowski [23] and later refined in Feynman's Lectures on Physics [24]. Experimental work on ratchet systems is nicely reviewed in [22], see also [25] for recent work on atomic systems. The interest in cold atoms for ratchet systems lies in the here possible realization of a Hamiltonian quantum ratchet system. A quantum mechanical ratchet for cold atoms can be thought of by building a sort of quantum barrier like the asymmetric optical potential described above, see Fig. 1.2a. A nondirected motion can be produced by rocking the ratchet potential forth and back, or alternatively flashing the ratchet on and off. The atoms spread over the whole lattice follow the dragging, but because of the asymmetry of the lattice the probability for tunneling into one direction is preferred. Consequently, the atoms start to move into the preferred direction of tunneling leading to a measurable current of atoms.

By such a periodic rocking no energy is added to the system since the energy contribution vanishes in the time average. The one-dimensional Hamiltonian of such a system is of the form

$$H(z, p, t) = \frac{p^2}{2M} + V(z)E(t), \quad (1.3)$$

where p is the atom's momentum, M the atomic mass, and $E(t+T) = E(t)$ is a periodic driving force. A necessary condition to observe the quantum ratchet effect is to break all relevant temporal and spatial symmetries of the system [26]. In a theoretical work concerning the Hamiltonian ratchet (1.3) with the lattice potential (1.1) and an ac-driving force $E(t) = E_1 \cos(2\omega_{ac}t) + E_2 \cos(4\omega_{ac}t + \theta)$, where ω_{ac} is the driving frequency, it was shown that directed transport can here be achieved if $\phi \neq 0, \pm\pi/2$ and $\theta \neq 0, \pm\pi/2$ [27].

Acknowledgement

We acknowledge financial support from the Deutsche Forschungsgemeinschaft.

References

1. F. Bloch, *Z. Phys.* **52**, 555 (1928)
2. N.W. Ashcroft, N.D. Mermin, *Solid State Physics* (Saunders College Publishing, New York, 1976)
3. M.H. Anderson, J.R. Ensher, M.R. Matthews, C.E. Wiemann, and E.A. Cornell, *Science* **269**, 198 (1995)
4. K.B. Davis, M.-O. Mewes, M.R. Andrews, N.J. van Druten, D.S. Durfee, D.M. Kurn, and W. Ketterle, *Phys. Rev. Lett.* **75**, 1687 (1995)
5. M.B. Dahan, E. Peik, J. Reichel, Y. Castin, and C. Salomon, *Phys. Rev. Lett.* **76**, 4508 (1996)

6. M. Cristiani, O. Morsch, J.H. Müller, D. Ciampini, and E. Arimondo, *Phys. Rev. A* **65**, 63612 (2002)
7. C. Orzel, A.K. Tuchman, M.L. Fenselau, M. Yasuda, and M.A. Kasevich, *Science* **23**, 291, 2386 (2001)
8. M. Greiner, O. Mandel, T. Esslinger, T.W. Hänsch, and I. Bloch, *Nature* **415**, 39 (2002)
9. M. Greiner, I. Bloch, O. Mandel, T.W. Hänsch, and T. Esslinger, *Phys. Rev. Lett.* **87**, 160405 (2001)
10. M. Greiner, O. Mandel, T. Esslinger, T.W. Hänsch, and I. Bloch, *Nature* **415**, 39 (2002)
11. R. Grimm, J. Söding, and Y.B. Ovchinnikov, *JETP Lett.* **61**, 367 (1995)
12. A. Görlitz, T. Kinoshita, T.W. Hänsch, and A. Hemmerich, *Phys. Rev. A* **64**, 11401 (2001)
13. C. Mennerat-Robilliard, D. Lucas, S. Guibal, J. Tabosa, C. Jurczak, J.-Y. Courtois, and G. Grynberg, *Phys. Rev. Lett.* **82**, 851 (1999)
14. P.R. Berman, B. Dubetsky, and J.L. Cohen, *Phys. Rev. A* **58**, 4801 (1998)
15. M. Weitz, G. Cennini, G. Ritt, and C. Geckeler, *Phys. Rev. A* **70**, 43414 (2004)
16. G. Ritt, C. Geckeler, T. Salger, G. Cennini, and M. Weitz, *Phys. Rev. A* **74**, 63622 (2006)
17. G. Cennini, G. Ritt, C. Geckeler, and M. Weitz, *Phys. Rev. Lett.* **91**, 240408 (2003)
18. C. Zener, *Proc. R. Soc. London A* **137**, 696 (1932)
19. Y. Gefen, E. Ben-Jacob, and A.O. Caldeira, *Phys. Rev. B* **36**, 2770 (1987)
20. Q. Niu, X.-G. Zhao, G.A. Georgakis, and M.G. Raizen, *Phys. Rev. Lett.* **76**, 4504 (1996)
21. T. Salger, C. Geckeler, S. Kling, and M. Weitz, arXiv:0707.1980
22. P. Reimann, *Physics Reports* **361**, 57 (2002)
23. M.v. Smoluchowski, *Physik. Zeitschr.* **13**, 1069 (1912)
24. R.P. Feynman, R.B. Leighton, and M. Sands, vol. 1, (Addison-Wesley, Reading, MA, 1963)
25. R. Gommers, M. Brown, and F. Renzoni, *Phys. Rev. A* **75**, 53406 (2007)
26. S. Flach, O. Yevtushenko, and Y. Zolotaryuk, *Phys. Rev. Lett.* **84**, 2358 (2000)
27. S. Denisov, L. Morales-Molina, S. Flach, and P. Hänggi, *Phys. Rev. A* **75**, 63424 (2007)